CONCRETE RESEARCH LETTERS
www.crl.issres.net Vol. 2 (4) – December 2011

Shear Strength of Self-compacting Concrete Containing Different Fillers and Coarse Aggregates

Mohamed A. Safan[c]
Department of Civil Engineering, Faculty of Engineering
Menoufai University, EGYPT

Abstract

An experimental investigation was conducted to evaluate the shear strength provided by different self-compacting concrete mixes proportioned using different fillers and coarse aggregates. A total of 28 simple beams without shear reinforcement were tested in flexure. The test parameters included the use of gravel versus crushed dolomite as coarse aggregates, the amount of longitudinal reinforcement and the composition and percentage of fillers. Dolomite stone powder with either silica fume or fly ash were used as fillers replacing cement aiming at reducing the cost of the mix and obtaining better performance. Test results indicated that the overall structural performance in terms of cracking pattern and shear strength was comparable in all mixes. The potentials of developing shear strength and post cracking shear resistance were better when gravel was used as coarse aggregate and when relatively high fractions of dolomite powder were used as cement replacement.

Keywords: shear strength; self-compacting concrete; common cements; dolomite powder; coarse aggregate type.

1. Introduction

Flexure members in reinforced concrete structures are designed to fail in a ductile manner. For this purpose, design codes set upper limits for the amount of longitudinal reinforcement to ensure yielding of steel before concrete reaches crushing strains. Sufficient web reinforcements are also arranged to prevent premature failures that may occur due to lack of shear strength. The shear strength provided by concrete is based on an average shear stress for design purpose. This shear strength is assumed to be the same for beams with and without web reinforcement and is taken as the shear causing inclined cracking [1]. The ACI-ASCE Joint Committee [2] described two types of inclined shear cracks. The first refers to "web-shear" cracks initiating near the mid-depth of an uncracked section and the second refers to "flexure-shear" cracks that is developed from the tip of an already existing flexure crack and propagates diagonally away from the adjacent support.

Shear failure mechanisms are rather complex due to the combination of stresses acting on different planes and redistribution of stress upon flexure cracking. However, shear transfer mechanisms in reinforced concrete beams without shear reinforcement are well documented for

[c] Corresponding Author: Mohamed A. Safan
Email: msafan2000@yahoo.com Telephone: +2010 919623 Fax: +20482328405

conventional concrete. According to the Joint ACI-ASCE Committee 445 [3] the shear resistance of concrete in such beams is due to: (i) uncracked concrete at the development of first shear crack or uncracked portions of cracked members, (ii) aggregate interlock between two slip surfaces (in a prominent diagonal crack) in the cracked portion of the beam as the protruding aggregates from either surface interlock and (iii) dowel action where the longitudinal steel reinforcement resists part of the shear displacement by dowel forces in the bar. The dowel force in the longitudinal reinforcement bar depends on the relative stiffness of the portion of the bar crossing the crack. The early work of Taylor [4] investigating normal concrete beams without web reinforcement showed that the shear strength is derived from the contribution of the compression zone (contribution between 20-40%), the aggregate interlock mechanism (contribution between 35-50%) and the dowel action of longitudinal reinforcement (contribution between 15-25%). Actually, these shear strength parameters influence each other; for instance, the aggregate interlock is influenced by the longitudinal reinforcement ratio and this component of shear strength is more significant if the cracks are narrow. Thus, higher percentage of longitudinal reinforcing steel which reduces the shear crack width would allow the concrete to resist more shear [5, 6].

Different shear failure modes may develop depending on the exact contribution of these strength parameters. Common shear failure patterns are shear-tension, shear compression, diagonal tension and arch-rib failures. While some of these modes can be violent with chunks of concrete thrown away, some can be relatively ductile and nonviolent. The sequence of events associated with each of these different failure modes is described in details in ref. [2].

The above arguments considering shear strength parameters and failure modes are well documented for conventional concrete types with regard to the enormous research in this area. However, a new technology utilizing the potentials of concrete and the advances in the manufacture of concrete admixtures produced a special type of concrete known as self-compacting concrete (SCC). This type of concrete has the ability to flow and fill the forms without using compaction equipment. Proper design of the mix provides sufficient viscosity preventing segregation tendency [7-10].

To achieve satisfactory combinations of high fluidity and stability, SCC requires high powder volumes at relatively low water/powder ratios with significant quantities of superplasticizers. The powder generally consists of a combination of Portland cement with one or more additions such as limestone powder, fly ash (FA), ground granulated blast furnace slag (GGBS) and/or condensed silica fume (SF). Therefore, strength tends to be governed as much by the type and proportion of powder addition than by the water/powder ratio [11].

There is some concern among designers that SCC may not be strong in shear due to lack of some of the mechanisms resisting shear, notably the aggregate interlock mechanism. Because of the presence of comparatively smaller amount of coarse aggregates in SCC, the fracture planes should be relatively smooth as compared with conventional concrete. Smooth fracture planes normally reduce the shear resistance of concrete by reducing the aggregate interlock between the fracture surfaces [12, 13].

The studies of Schiessl and Zilch [14] on the contribution of aggregate interlock to the shear strength of cracked sections considered the shear strength of the interface between prefractured surfaces under varying levels of normal stress. It was found that for similar concrete strength, the shear strength for any given normal stress was about 10% lower in case of SCC due to smoother crack surfaces.

Boel et al. [15] studied the shear strength for both SCC and normally vibrated concrete (NVC) mixes used in casting beams without web reinforcement with variable shear span-to-depth ratio. SCC mixes incorporated only limestone filler. The filler/powder ratios were as high as 50 percent and the characteristic strength of the mixes ranged between 50 and 60 MPa. The test results showed that the beams cast with SCC had about 3 percent lower shear capacity compared to those cast with NVC.

The influence of the coarse aggregate type on the compressive strength of SCC mixes was analyzed by Domone [11] utilizing data collected from many published studies. The crushed aggregate mixes have a higher cube compressive strength compared to uncrushed gravel mixes with average 4.0 MPa difference between the two best-fit curves. This difference is less than typical values of 7.0 MPa assumed in the design of normally vibrated concrete according to the BRE design method [16]. It seems that the influence of coarse aggregate type was less significant in SCC mixes compared to conventional concrete.

Lachemi et al. [17] studied the shear resistance of normally vibrated concrete (NVC) versus SCC mixes in simple beams without shear reinforcements. The mixes were proportioned using ordinary Portland cement contents of 405-490 kg/m^3 as the only powder material. The test parameters included the amount of coarse aggregates (less content in SCC mixes), the MNS of coarse aggregates and the shear span-to-depth ratio. It was found that an increase in the size of coarse aggregate from 12 to 19 mm in SCC mixes decreased the shear capacity of concrete (V_c) and on the other hand, increased the ultimate shear resistance (V_u). Keeping the maximum size of coarse aggregate constant, SCC mixes with lower coarse aggregate content showed similar concrete shear resistance in the pre-cracking stage as compared with NVC. On the other hand, lower post-cracking shear resistance in SCC compared with NVC was observed due to less aggregate interlock and dowel action with regard to the lower quantity of coarse aggregate.

Hassan et al. [18, 19] tested simple beams without web reinforcements to study the influence of the beam depth, the longitudinal reinforcement ratio and the coarse aggregate content. The coarse aggregate content was higher in NVC mixes compared to SCC mixes that was proportioned using ordinary Portland cement and slag cement at 315 and 135 kg/m^3 contents, respectively. SCC beams showed lower ultimate shear loads compared to their NVC counterparts and the shear strength reduction was higher in deeper beams with lower longitudinal steel ratios. The ultimate shear loads were less by 4-8 percent in SCC beams compared to similar NVC beams with 2.0 percent reinforcement ratio irrespective of the beam depth. This ratio increased to 14-17 percent in deeper beams with lower reinforcement ratio of 1.0 percent. This result was attributed to the role of steel in limiting the cracking width and consequently increasing the shear resistance due to aggregate interlock.

2. Design Equations for Shear Strength:

Current design codes adopted different equations for the shear strength in concrete beams without web reinforcement. The equations adopted by the ACI 318-95 code [1] and JSCE code [20] had been verified by many authors [15, 18, 19, 21] and were found to provide accurate predictions for shear strength.

The ACI 318-95 [1] code presented a detailed equation (Eq. (1) based on SI units) for calculating the concrete shear strength V_c as the force causing significant inclined cracking:

$$V_c = (0.158\, f_c^{1/2} + 17.24\, r\, V_u\, d / M_u)\, bd \leq 0.28\, f_c^{1/2}\, bd \qquad (1)$$

In which b is the width of the beam, d is the effective depth, r is the reinforcement ratio and V_u and M_u are the factored shear force and moment occurring simultaneously at the section considered. Seeking for simplicity of application, Eq. (1) is allowed to be reduced to the following form (based on SI units):

$$V_c = 0.166\, f_c^{1/2}\, bd \qquad (2)$$

Niwa [22] proposed Eq. (3) for estimating V_c and this equation was the basic version of the current JSCE-86 code equation, Eq. (4) (based on SI units):

$$V_c = 0.2\,(0.75+ 1.4\,d/a)\;\; f_c^{1/3}\,(1000/d)^{1/4}\,(100r)^{1/3}\,bd \qquad (3)$$

$$V_c = 0.2\;b_d\,b_p\,b_n\;\; f_c^{1/3}\,bd \qquad (4)$$

where $b_d = (1000/d)^{1/4} \leq 1.5$, $b_p = (100r)^{1/3} \leq 1.5$ and b_n a factor not more than 2.0 to account for an acting axial compressive force.

3. Experimental study

Twenty eight beams without web reinforcement were tested to study shear strength and failure mechanisms. The beams were designed to have adequate resistance against flexure failure. Fourteen SCC mixes were used to cast the test specimens that had the same cross section with two different reinforcement ratios. Seven mixes incorporated natural gravel as coarse aggregate, while crushed dolomite was used in the other seven mixes. Thus, the experimental work was intended to study the effect of the following parameters (i) the composition and amount of the filler used as Portland cement replacement, (ii) type of the coarse aggregates used (natural gravel versus crushed dolomite) and (iii) variation in the main reinforcement ratio. The concrete mixes were designated by the type of the coarse aggregate (D: Dolomite and G: Gravel) and the concrete mix number (1-7). The test beams were further designated by a number (10 or 12) indicating the diameter of the longitudinal steel rebars. Test beams were reinforced with two bottom rebars of 10-mm diameter (reinforcement ratio ρ = 1.16%) or 12-mm rebars (reinforcement ratio ρ = 1.68%). Thus, a beam designated as D2/10 is cast using crushed dolomite as coarse aggregate in mix No. 2 and has a reinforcement ratio of 1.16%.

3.1 Materials

Locally produced Portland cement (CEMI: 52.5 N) conforming to the requirements of BS EN 197-1:2000 [23] with specific gravity of 3.16 and Blain fineness of 4850 cm^2/gm was used. Locally produced densified silica fume (SF) was delivered in 20-kg sacks. According to the manufacturer, the powder had a specific gravity of 2.2, specific surface area of 17 m^2/gm. Imported class (F) fly ash meeting the requirements of ASTM C618 [24] with a specific gravity of 2.1 was used. The particle size distribution curve, Fig. (1), shows that 90 percent by weight of ash passes through the 45-μm sieve. The dolomite powder was obtained from a local plant for ready-mix asphalt concrete. The production process includes heating (is heating correct?) the crushed dolomite used as coarse aggregate and sieving the aggregates to separate the different sizes. A small fraction of the powder that passes through sieve No. 50 (300 μm) is used in the mix, while most of the powder is a by-product. The powder had a light brownish colour and specific gravity of 2.75. Sieving six random samples of the powder showed that the average passing percentage through the 45-μm sieve was 63 percent, Fig. (1).

Natural sand having a fineness modulus of 2.65 and a specific gravity of 2.67 was used. Crushed dolomite (specific gravity of 2.65 and crushing modulus of 18 percent) and natural gravel (specific gravity of 2.67 and crushing modulus of 15 percent) were used as coarse aggregates. The maximum nominal size of coarse aggregates was 19 mm. The grading of the used aggregates is shown in Fig. (1). A novel superplasticizer of modified polycarboxylates was used in all mixes. This admixture is a turbid aqueous solution with a specific gravity of 1.08 and conforms to ASTM C494 (types F and G) [25]. High tensile deformed steel rebras with nominal diameters of 10 and 12 mm were used as tension reinforcement with yield strength of 555 and 430 MPa, respectively.

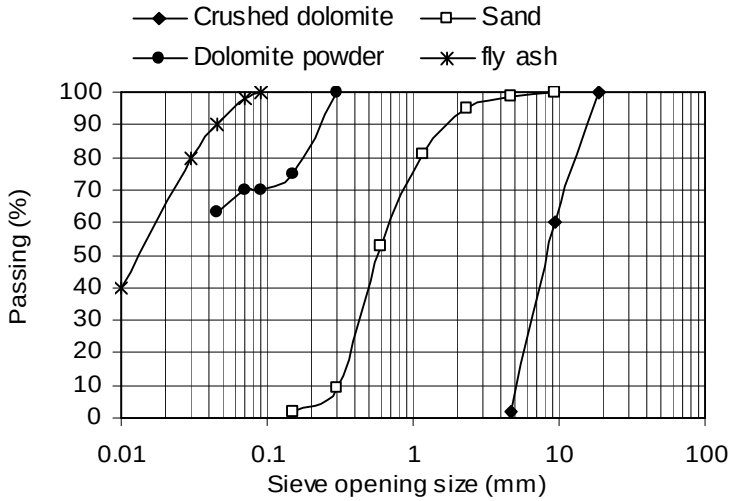

Figure 1. Grading of aggregates and mineral admixtures

3.2 Concrete mix proportions

In all mixes, the fine-to-coarse aggregate ratio was 1.13, the total content of powders (cement and fillers) was 500 kg/m^3, the HRWR dosage was fixed at 8.5 kg/m^3 for dolomite mixes (1.7% by weight of powders) and 6.5 kg/m^3 for gravel mixes (1.3% by weight of powders). The water content was determined by trail mixes to obtain a consistent mix with the required fresh rheological properties. The water-to-powder ratio (w/p) ranged between 0.32 and 0.35 depending on the composition and content of the filler as reported in Table (1). The composition of the filler replacing cement in mixes (D1-D7) incorporating dolomite and (G1-G7) incorporating gravel is shown in Table (1). All mixes incorporated dolomite powder (DP) replacing from 10 to 30 percent of cement by weight. Either silica fume (SF) or fly ash (FA) was used along with the dolomite powder in some mixes replacing 10 percent of cement. The constituents of the selected SCC mixes are given in Table (1).

TABLE 1: CONCRETE MIX PROPORTIONS

Mix	Powder Contents, kg/m^3				w/p
	C	DP	SF	FA	
D1, G1	500	--	--	--	0.32
D2, G2	450	50	--	--	0.33
D3, G3	400	100	--	--	0.34
D4, G4	350	100	50	--	0.34
D5, G5	300	150	50	--	0.35
D6, G6	350	100	--	50	0.34
D7, G7	300	150	--	50	0.35

HRWR dosage: 1.7% (D-mixes) and 1.5% (G-mixes) of powder by weight

3.3 Test specimens

A 60-liter mixer was used in mixing concrete. The fine materials were thoroughly mixed before adding the coarse aggregate. The whole amount of water was then added and mixing continued for two minutes. The admixture was slowly added during mixing that continued for further five minutes. The rheological properties were measured in terms of slump flow and the V-funnel time as in Table (2). A 45-liter batch was used to cast one beam (100x150x1100) mm, three cylinders (100x200) mm and three prisms (100x100x500) mm. The cylinders and prisms were tested before testing the beams to determine the concrete compressive strength, f_{cy}, and the modulus of rupture, f_r for each mix. Results are shown in Table (2). Tight wooden forms were used to cast the test beams.

The inside faces of the forms were greased to prevent water absorption. The reinforcement was carefully placed inside the forms and concrete was cast from one side without any compaction. The specimens were stripped after 24 hours and cured under wet cloth for 7 days and then allowed to dry in the laboratory atmosphere.

TABLE 2: RHEOLOGICAL AND HARDENED PROPERTIES OF SCC MIXES

Mix	f_{cy} (MPa)		f_r (MPa)		Slump flow (mm)		V-funnel t_o (sec.)	
	D	G	D	G	D	G	D	G
D1, G1	75	56	5.7	4.7	700	720	6.0	5.9
D2, G2	64	47	5.8	4.7	650	670	5.9	5.9
D3, G3	53	37	4.9	4.1	610	640	5.3	5.5
D4, G4	55	37	5.2	4.0	660	655	5.3	5.3
D5, G5	51	33	4.9	4.1	640	650	4.9	5.0
D6, G6	48	30	5.0	4.5	670	680	4.9	4.8
D7, G7	41	26	5.0	3.4	650	650	5.0	4.9

After 28 days of casting, the test beams were painted in white to facilitate detection of the cracks. The beams were tested under 4-point loading until failure, Fig. (2). The loading configuration was arranged keeping the shear span constant at 350 mm yielding a shear span-to-depth ratio of 2.6. The load was applied at constant increments of 2.0 kN utilizing 100 kN capacity hydraulic flexure machine. The mid-span deflection was measured using a dial gage and the cracks were traced after each load increment.

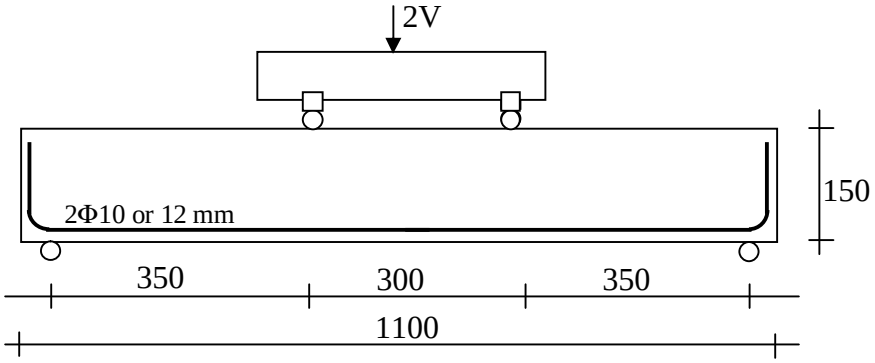

Figure 2. Loading configuration (Dimensions in mm)

4. Test Results and Discussion

4.1 Mechanical properties of SCC mixes

SCC mixes were proportioned using 19-mm crushed dolomite and natural gravel as coarse aggregates. The Portland cement was replaced by relatively large amounts of dolomite powder. The replacement ratios were 10% and 20% by weight of cement and further increased to 20% and 30% along with 10% of either silica fume or fly ash. Thus, the total replacement ratios ranged from 10 % to 40 %. Fig. (3) is a plot of the concrete compressive strength f_{cy} values reported in Table (2) against the total percentage of cement replacement. The plot shows a continuous decrease of strength as the total replacement ratio increased. It can be seen that the use of 10% silica fume was effective in stopping severe reduction of the compressive strength at higher replacement ratio of dolomite powder. On the other hand, using 10% fly ash helped only to decrease the strength reduction rate, yet the compressive strength continued to decrease. The compressive strength of gravel mixes was less than that of the crushed dolomite mixes despite the higher intrinsic strength of gravel in terms of crushing modulus. The lower compressive strength of a given mix containing gravel is attributed to lower paste-aggregate bond

strength due to the relatively smoother surface of the gravel particles. It worth mentioning that the compressive strength was less by about 17 MPa in all mixes when natural gravel was used instead of crushed dolomite. This result suggested that the paste-aggregate bond characteristics were not negatively affected due to cement replacement in all the investigated mixes.

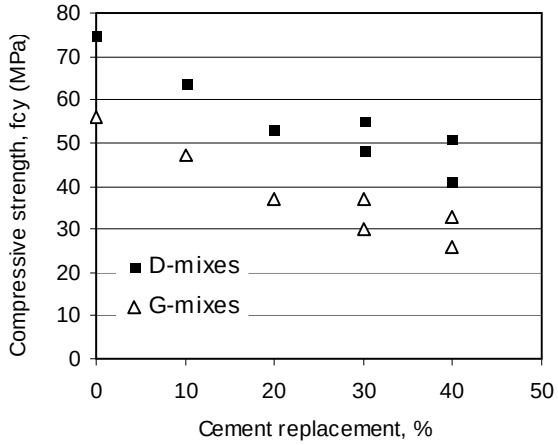

Figure 3. Compressive strength for different replacement ratios

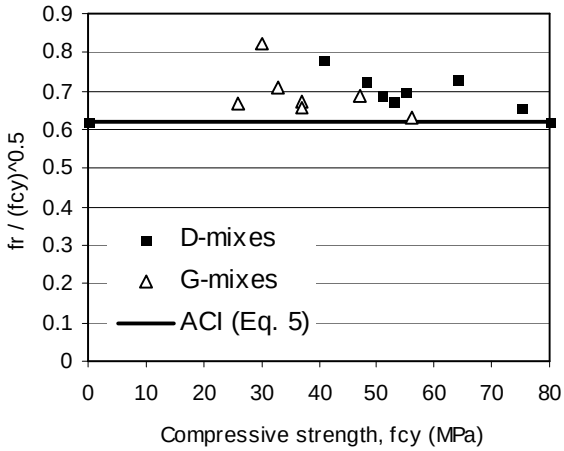

Figure 4. Normalized fracture modulus versus compressive strength

Fig. (4) shows a plot of the normalized fracture modulus (the fracture modulus f_r values reported in Table (2) divided by the square root of the characteristic strength f_{cy}) and a plot of the ACI-318 code equation for predicting the fracture modulus (Eq. (5) – SI units):

$$f_r = 0.622 \, (f_{cy})^{1/2} \qquad (5)$$

Fig. (4) shows that the fracture modulus was safely predicted using Eq. (5). It can be seen that the intrinsic fracture modulus tended to increase in both gravel and dolomite mixes having lower compressive strength. This trend is consistent with the previous suggestion that the paste-aggregate bond characteristics were not negatively affected due to cement replacement.

4.2 Cracking and failure behavior

Fig. (5) shows the cracking patterns for test beams at failure. The total amount of load applied by the testing machine (2V) is written close to the point the crack reached at this load in order to trace the propagation of cracking. All beams cracked in the early stages of loading in the maximum moment region within the middle third of the beam. Those fine flexure cracks propagated upwards with loading and new flexure cracks appeared in the shear spans. Failure took place due to shear in all beams as planned. However, two distinct failure modes were observed:

(i) Diagonal tension failure: this failure mode took place in two beams (D1/10 and D1/12) that satisfied the requirements of this type of failure [2]. While no web-shear cracks were observed, the outer most flexure crack in the shear span propagated diagonally towards the loading point. Immediately prior to failure, a secondary crack stretched from the lower part of the crack along the steel rebars and the upper of the crack moved towards the loading point at a flat slope. Failure was sudden and violent due to splitting of concrete along the steel associated with concrete crushing in the compression zone. This type of

failure could be related to the high characteristic strength of mix D1 (75 MPa). Actually, this type of failure is not common in normal strength concrete and is considered particular to high strength concrete [26].

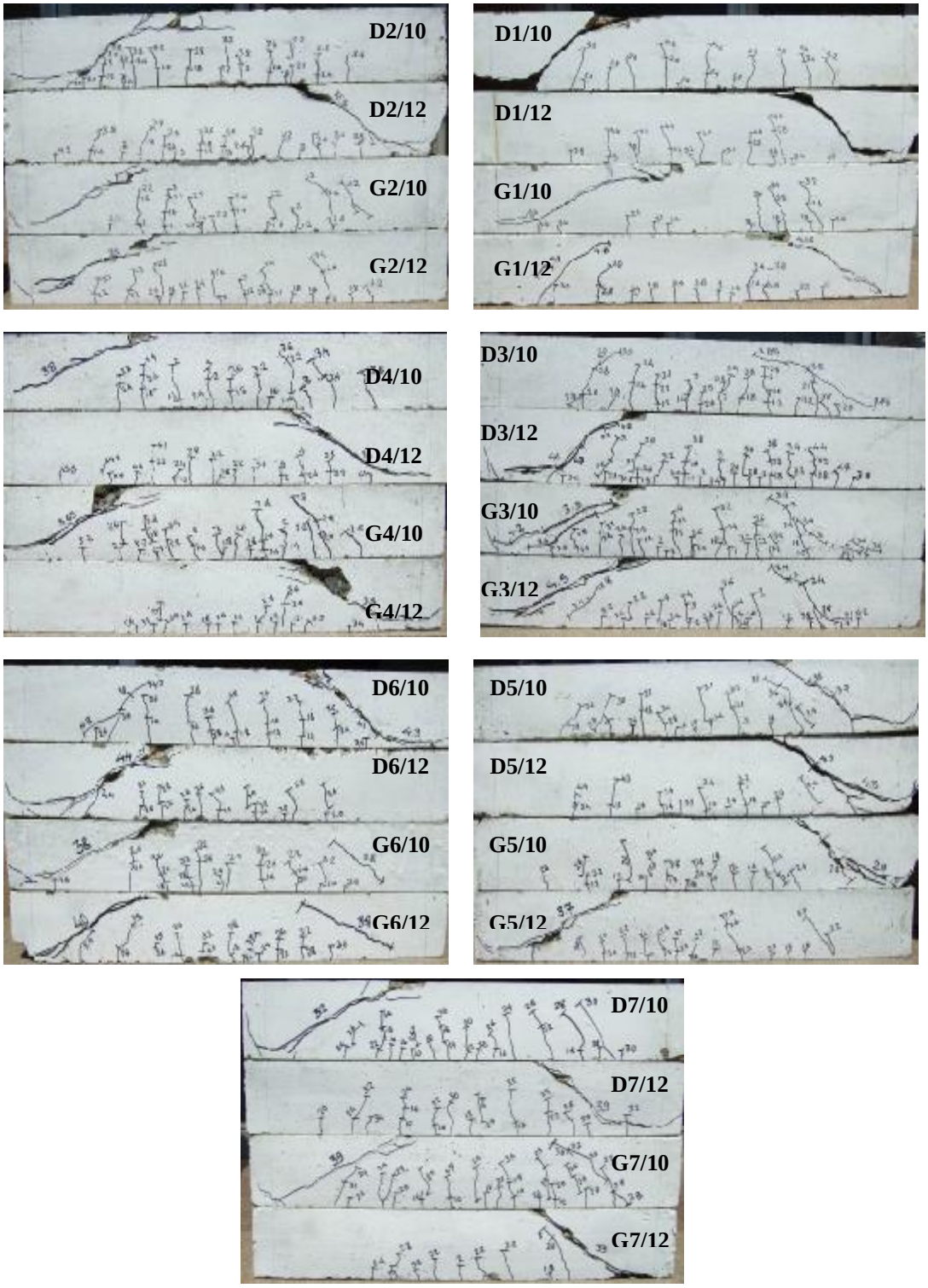

Figure 5. Cracking patterns at ultimate failure loads

(ii) Arch-rib failures: the rest of test beams failed due to arch-rib failure associated with concrete failure along the compression strut (beam G7/12) or concrete crushing in compression crown in all other beams. In beam G7/12 the initial flexural cracks extended

only slightly above the steel reinforcement. As load increased, a web shear crack developed in the shear region and extended from the support to the adjacent loading point. Failure took place due to concrete crushing along the compression strut in a nonviolent manner. The rest of the beams behaved similarly, yet a longitudinal crack developed along the reinforcement as if a splitting failure would occur. Final failure occurred due to concrete crushing under the loading point in a nonviolent manner.

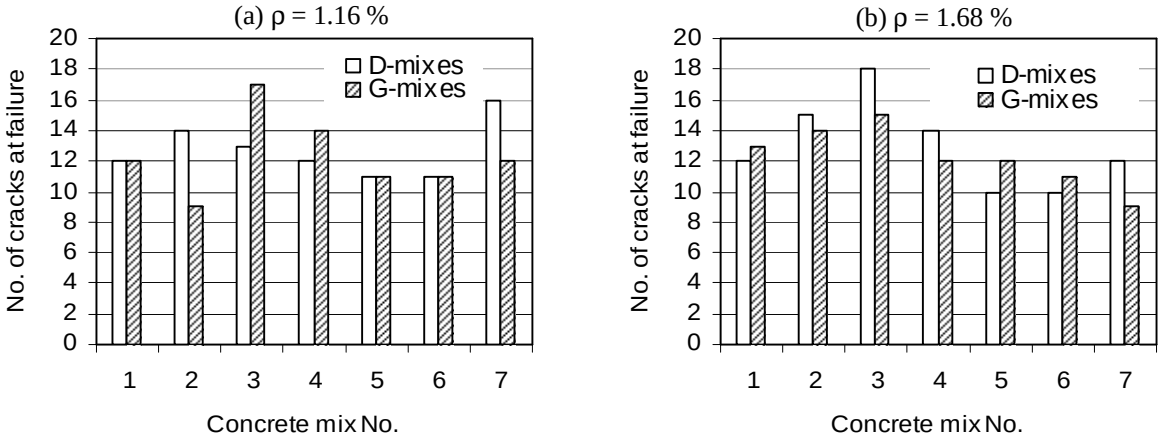

Figure 6. Number of cracks at failure for different reinforcement ratios

In general, the increase of the reinforcement ratio restricted the extension of most of the cracks compared to the corresponding beams with lower reinforcement ratio. Excluding web cracks, the number of flexure cracks at failure is shown in Fig. (6). It can be seen that the number of flexure cracks increased in all beams cast using mix 3 incorporating 20 percent of dolomite powder compared to their counterpart control beams cast using mixes D1 and G1. The increased number of flexure cracks reflects enhanced steel-concrete bond characteristics. This result can be linked to the observed increased stickiness of the mixes incorporating dolomite powder suggesting better uniformity in the interfacial transition zone around the reinforcing bars. Further addition of either silica fume or fly ash reduced the stickiness of the mixes and the number of cracks was either unchanged or higher compared to control beams. The number of cracks in beams G2/10 and G7/12 was notably lower due to misplacing of the two longitudinal rebras close to one side of the beam.

Visual inspection of the shear failure planes in the tested beams showed that these planes were smooth passing through the coarse aggregate particles in all beams incorporating crushed dolomite. Thus, it was evident that the paste-aggregate bond strength provided sufficient resistance preventing coarse aggregate debonding independent of the composition of the powder. On the other hand, failure planes were rough when gravel was used as coarse aggregate. Debonding of gravel particles was observed in all beams due to the high intrinsic strength of gravel and relatively lower paste-aggregate bond strength. It was common that the debonding particles in one face across failure planes left 2-8 mm deep notches on the opposite face. The failure plans were consequently irregular and rough allowing for developing the aggregate interlock mechanism. The amount of aggregate interlock contribution to the overall shear resistance depended on the aggregate penetration depth across the shear failure plane and the intensity and distribution of the debonding particles that was found to differ randomly from one beam to another.

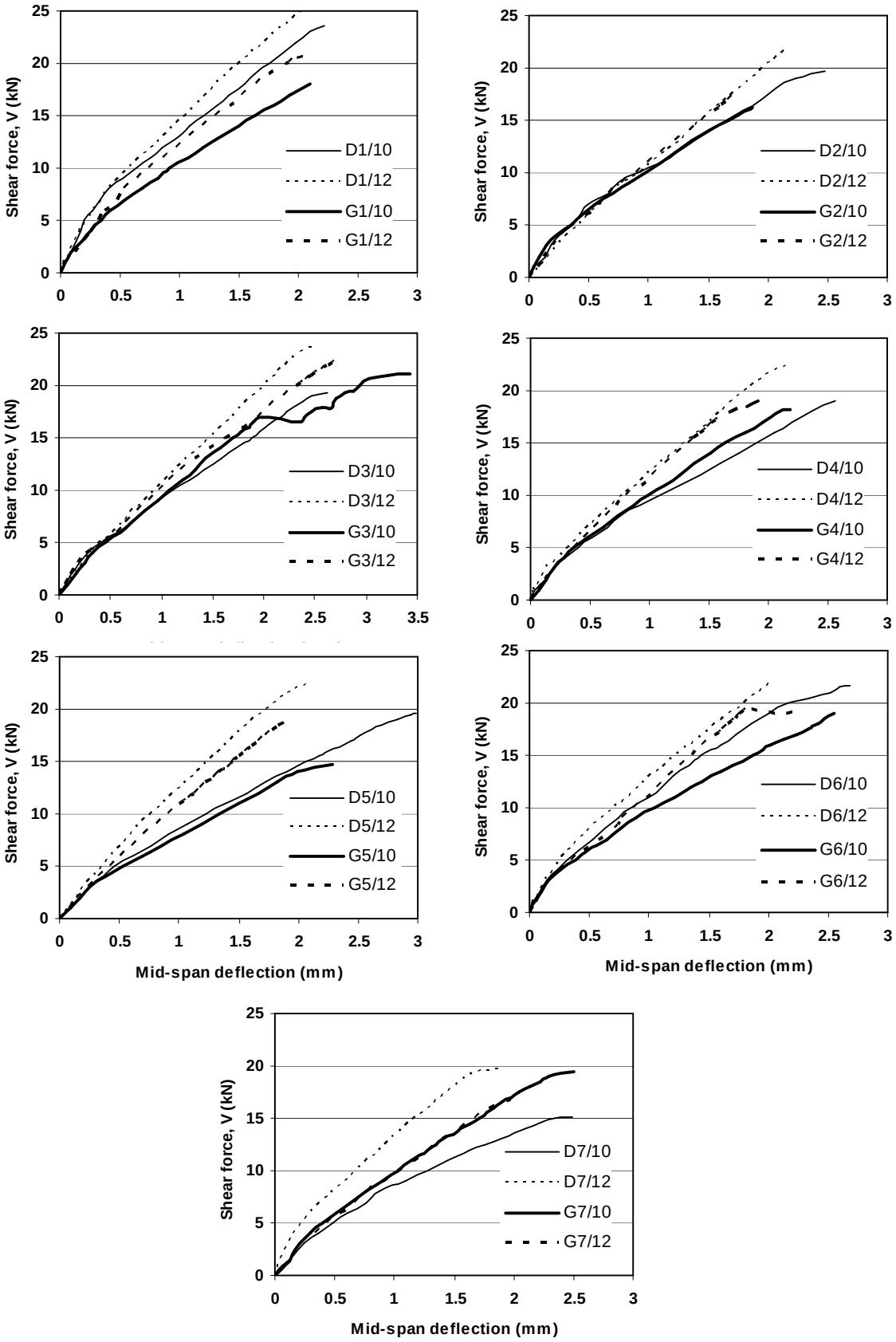

Figure 7. Load mid-span deflection relationships

4.3 Load – deflection response

Fig. (7) shows the applied shear load versus mid-span deflection curves for test beams throughout the whole course of loading. All curves showed a change of slope at first flexure cracking load. The cracking loads reported in Table (3) tend to increase with the increase of the fracture modulus. Increasing the reinforcement ratio from 1.16% to 1.67 % did not significantly influence the flexure cracking loads. For a given reinforcement ratio, it seems that the coarse aggregate type did not significantly influence the load-deflection response. However, the beams containing dolomite showed a slightly improved stiffness compared to similar beams containing gravel. On the other hand, the influence of the reinforcement ratio was significant in increasing the stiffness due to the reduced deflection at a given load level as the extension of cracks was restricted. Most of the beams showed a linear response after first cracking and failed suddenly due to the formation of a single-failure diagonal crack in one side. Two beams (G3/10) and (G6/12) demonstrated more than one peak before failure. This was attributed to the formation of additional diagonal cracks before failure as can be seen in Fig. (5).

TABLE 3: EXPERIMENTAL AND THEORTICAL SHEAR LOADS

Beam	V_u (kN)	$V_{norm.}$	V_{fc} (kN)	code based shear strength V_c (kN)				V_u / V_{sc}
				Eq. (1)	Eq. (2)	Eq. (3)	Eq. (4)	
D1/10	23.7	0.20	8.0	19.4	21.2	25.5	18.0	1.00
D1/12	25.3	0.22	9.0	19.4	22.4	28.8	20.3	1.00
G1/10	18.0	0.18	6.0	16.8	18.7	23.1	16.3	1.13
G1/12	20.8	0.21	7.0	16.8	19.9	26.1	18.4	1.10
D2/10	19.8	0.18	7.0	18.0	19.8	24.2	17.0	1.00
D2/12	21.8	0.20	7.0	18.0	21.0	27.3	19.2	1.00
G2/10	16.3	0.18	5.0	15.4	17.3	21.8	15.4	1.36
G2/12	17.5	0.19	6.0	15.4	18.5	24.6	17.4	1.35
D3/10	19.3	0.20	6.0	16.3	18.2	22.7	16.0	1.20
D3/12	23.7	0.24	6.0	16.3	19.4	25.6	18.1	1.18
G3/10	21.2	0.26	5.0	13.7	15.7	20.1	14.2	1.41
G3/12	22.5	0.27	5.0	13.7	16.9	22.7	16.0	1.50
D4/10	19.0	0.19	6.0	16.7	18.5	23.0	16.2	1.12
D4/12	22.4	0.22	6.0	16.7	19.8	26.0	18.3	1.04
G4/10	18.3	0.22	5.0	13.7	15.7	20.1	14.2	1.40
G4/12	19.0	0.23	5.0	13.7	16.9	22.7	16.0	1.00
D5/10	19.6	0.2	6.0	16.0	18.0	22.4	15.8	1.31
D5/12	22.5	0.23	6.0	16.0	19.1	25.3	17.8	1.32
G5/10	14.7	0.19	4.0	12.9	15.0	19.4	13.7	1.34
G5/12	18.8	0.24	4.0	12.9	16.2	21.9	15.4	1.25
D6/10	21.7	0.23	5.0	15.6	17.5	22.0	15.5	1.14
D6/12	22.1	0.24	6.0	15.6	18.7	24.8	17.5	1.23
G6/10	19.0	0.26	4.0	12.3	14.4	18.8	13.2	1.36
G6/12	20.1	0.27	4.0	12.3	15.6	21.2	14.9	1.06
D7/10	15.1	0.19	6.0	14.4	16.4	20.8	14.7	1.08
D7/12	19.8	0.25	5.0	14.4	17.6	23.5	16.6	1.10
G7/10	19.5	0.28	5.0	11.4	13.6	17.9	12.6	1.34
G7/12	16.8	0.24	5.0	11.4	14.8	20.2	14.3	1.29

V_u: ultimate shear force, $V_{norm.}$: normalized shear stress ($V_u/bd\sqrt{f_{cy}}$), V_{fc}: shear force at first flexure cracking, V_{sc}: shear force at first shear crack

4.4 Shear strength

The experimental ultimate shear loads V_u are reported in Table (3). Simplified code design equations, for instance Eq. (2), assume that the shear strength is proportional with the square root of the compressive strength f_{cy}. With regard to the wide range of the

compressive strength of the investigated mixes (26-75) MPa, it was convenient to analyze the shear strength based on normalized shear strength $V_{norm.}$:

$$V_{norm.} = V_u / bd\,(f_{cy})^{1/2} \qquad (6)$$

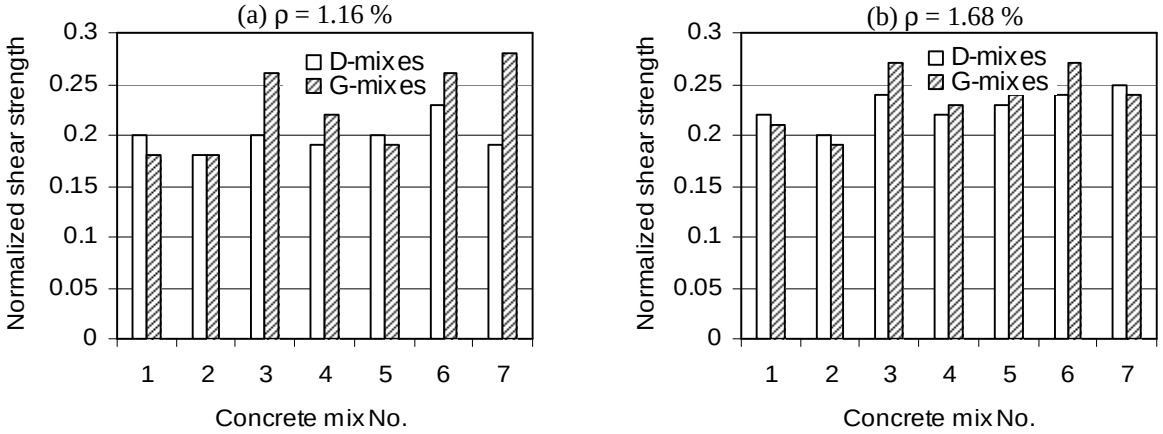

Figure 8. Normalized shear strength

The values of $V_{norm.}$ are reported in Table (3) and plotted in Fig. (8) against the concrete mix number. For the lower reinforcement ratio (1.16%), the analysis of the results showed that the normalized shear strength ranged between 0.18 to 0.23 with an average of 0.2 for mixes (2-7) containing dolomite and ranged between 0.18 and 0.28 with an average of 0.23 for mixes containing gravel. The average values of 0.2 and 0.23 were zero and 28 percent higher than the normalized shear strength of the corresponding control beams cast using mixes D1 and G1. For the higher reinforcement ratio (1.68%), the analysis of the results showed that the normalized shear strength ranged between 0.20 to 0.25 with an average of 0.23 for mixes (2-7) containing dolomite and ranged between 0.19 and 0.27 with an average of 0.24 for mixes containing gravel. The average values of 0.23 and 0.24 were 5 and 14 percent higher than the normalized shear strength of the corresponding control beams cast using mixes D1 and G1. It can be shown that beams G3/10, G7/10 and G3/12 achieved the highest normalized shear strengths of 0.26, 0.28 and 0.27, respectively. These values were 44%, 55% and 29% higher than the normalized shear strength of the corresponding control beams. Actually, it was surprising that beams G3/10 and G3/12 cast with 37 MPa concrete (66% of the control compressive strength of mix G1) achieved ultimate shear loads that were 18% and 8% higher than the control beams G1/10 and G1/12, respectively. Also, beam G7/10 cast with 26 MPa concrete (46% of the control compressive strength of mix G1) achieved an ultimate shear load that was 8% higher than the control beam G1/10. This interpretation of tests results demonstrated that the gravel mixes containing relatively high fractions of dolomite powder replacing cement have higher potentials for developing shear strength compared to other mixes.

The results reported in Table (3) show that the normalized shear strength increased by an average of 15% as the reinforcement ratio increased from 1.16% to 1.67% in mixes (1-7) containing dolomite. The corresponding ratio was 10% in mixes (1-6) containing gravel given that the strength of beam G7/12 that failed prematurely due to misplacing of the steel rebars was not taken into account.

The ratios of the ultimate shear load to the shear force at first shear cracking V_u/V_{sc} for test beams are reported in Table (3). The first shear cracking load was determined by visual inspection during testing associated with either web or flexure-shear cracking. The ratio V_u/V_{sc} indicates the post-cracking shear resistance of concrete beams due to aggregate

interlock and dowel action. This ratio ranged from 1.0 to 1.32 with an average of 1.12 for mixes (1-7) containing dolomite. The corresponding ratios for mixes (1-7) containing gravel ranged from 1.1 to 1.5 with an average of 1.28. The highest ratios were recorded for beams G3/10 and G3/12 containing gravel and 20% of dolomite powder replacing cement. These ratios shows that the beams containing gravel and relatively high fraction of dolomite powder demonstrated superior post-cracking shear resistance compared to similar beams containing dolomite.

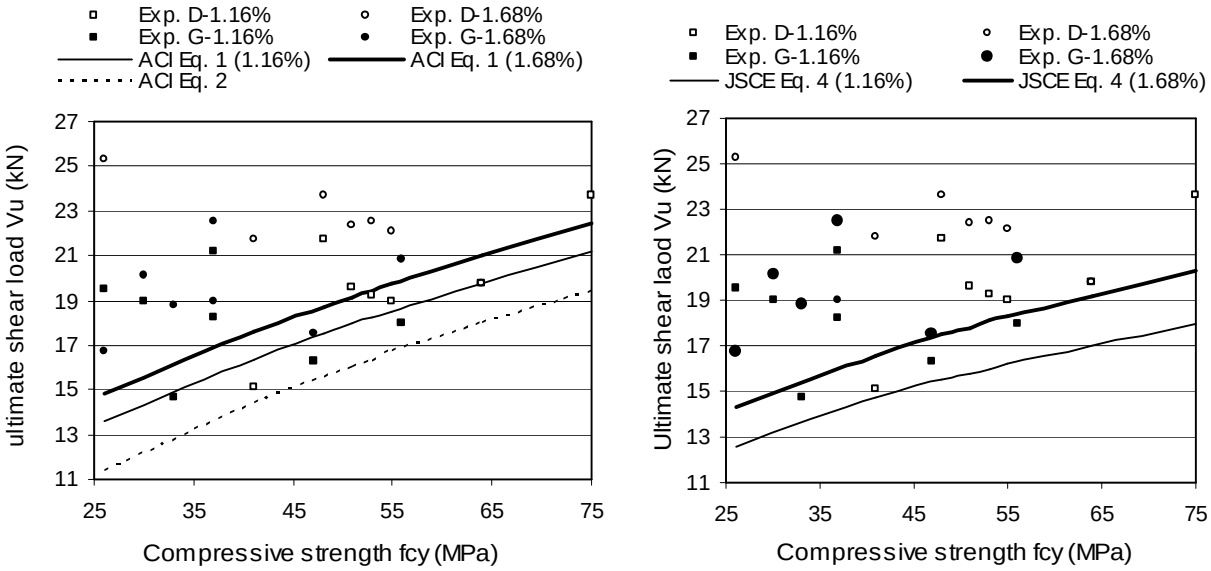

Figure 9. Experimental ultimate shear loads and verification of code based design equations

4.5 Verification of design equations

The shear strength V_c associated with significant concrete shear cracking was predicted for the test beams applying different code design equations (Eq. 1-4) and the calculated ultimate shear loads were reported in Table (3). Fig. (9) shows graphical representation of Eqs (1-3) against the experimental ultimate shear loads V_u. It can be seen that Eq. (2) representing a simple formula adopted by the ACI 318 code [1] was the most conservative in predicting the ultimate loads. The more detailed ACI Eq. (1) provided more accurate predictions. While the predictions were safe for the higher reinforcement ratio (1.68%), only three beams with reinforcement ratio 1.16% were overestimated by only 3 to 8 percent. Eq. (4) proposed by the recent version of the Japanese code, JSCE [20], provided safe predictions all beams. Eq. (3) proposed by Niwa was found to overestimate the ultimate shear loads and were found to be unsafe for shear failure loads within the scope of the described work.

5. Conclusions

The current work aimed to investigating the shear behavior of simple beams without web reinforcement cast using different mixes of self-compacting concrete. The mixes incorporated relatively high fractions of dolomite powder replacing Portland cement aiming at reducing the production cost. The test parameters included the composition of the fine materials, coarse aggregate type and reinforcement ratio. The beams were loaded till failure and the behavior was analyzed in terms of cracking and failure patterns, load-deflection response and shear resistance. The adequacy of the current design code based equations was checked. Based on the available test results and analysis, the following conclusions could be drawn:

1. The compressive strength was gradually reduced by increasing the percentage of dolomite powder replacing Portland cement. The use of 10% silica fume was effective in reducing the amount of strength reduction.
2. The structural performance of test beams cast with mixes incorporating 20% of dolomite powder was superior compared to the corresponding control beams without cement replacement. While the stiffness was comparable, the cracks at failure were more closely spaced and the ultimate shear loads were even higher when gravel was used as coarse aggregate. The increased number of cracks at failure was attributed to better steel –concrete bond characteristics with regard to the increased stickiness of the concrete mix.
3. The test beams containing gravel rather than crushed dolomite as coarse aggregate have better potentials to develop higher post-cracking shear resistance due to the development of aggregate interlocking mechanisms.
4. Test beams incorporating crushed dolomite sustained higher ultimate loads compared to their gravel counterparts due to higher compressive strength. However, the normalized shear strength of more than half of the gravel beams were higher compared to their dolomite counterparts. The capability of gravel beams to develop interlocking mechanisms and post shear cracking resistance compensates the influence of lower compressive strength.
5. Adding either 10 percent silica fume or fly ash improved the self-consolidating performance of the mixes by increasing the fluidity of the mixes. While the cracking patterns were not further improved by these additions, the normalized shear resistance was higher than that of the corresponding control beams.
6. The stiffness of test beams was not significantly influenced by the coarse aggregate type. On the other hand, the stiffness was significantly higher as the reinforcement ratio increased due to restricting the extension of flexure cracks.
7. The experimental ultimate shear loads were safely estimated by the current ACI 318 and the Japanese code design equations.

References

[1] ACI Committee 318, *Building Code Requirements for Reinforced Concrete*. ACI-95 and commentary ACI 318R-95, 1995: 369 p.

[2] Joint ACI-ASCE Committee 426, *Shear Strength of Reinforced Concrete Members*. Proceedings, ASCE, **99** (ST6), 1973: pp. 1148-1157.

[3] Joint ACI-ASCE Committee 445., *Recent Approaches to Shear Design of Structural Concrete*. ASCE Journal of Structural Division, **124** (2), 1998: pp. 1375–1417.

[4] Taylor, H. P., *The Fundamental Behavior of Reinforced Concrete Beams in Bending and Shear*. ACI SP-42, Detroit, 1974: pp. 43-77.

[5] Bentz, E. C., *Empirical Modeling of Reinforced Concrete Shear Strength Size Effect for Members Without Stirrups*. ACI Structural Journal, **102**, 2005: pp. 232–241.

[6] Tompos, E. J. and Frosch, R. J., *Influence of Beam Size, Longitudinal Reinforcement, and Stirrup Effectiveness on Concrete Shear Strength*. ACI Journal, **99** (5), 2002: pp. 559–567.

[7] Okamura, H.; Ouchi, M., *Self-compacting Concrete*. Journal of Advanced Concrete Technology, **1**, 2003: pp. 5-15.

[8] Okamura, H. and Ozawa, K., *Mix-design for Self-compacting Concrete* Concrete Library of JSCE, **25,** 1995: pp. 107-20.

[9] ACI Committee 237, *Self-consolidating Concrete*. ACI 237R-07, 2007: 34 p.

[10] Bouzoubaâ, N.; Lachemi, M., *Self-compacting Concrete Incorporating High Volumes of Class F Fy Ash: Preliminary Results* Cement Concrete Research, **31** (3), 2001: pp. 413–20.

[11] Domone, P. L., *A Review of the Hardened Mechanical Properties of Self-compacting Concrete*. Cement and Concrete Composites, **29**, 2007: pp. 1-12.

[12] Khayat, K. H.; Manai, K.; and Trudel, A., *In Situ Mechanical Properties of Wall Elements using Self-consolidating Concrete*. ACI Materials Journal, **94**(6), 1997: pp. 491–500.
[13] Zarais, P. D. and Papadakis, G. C, *Diagonal Shear failure and size effect in RC beams Without Web Reinforcement*. ASCE J., Struct. Div., **127**(7): 2001: pp. 733–741.
[14] Schiessl, A. and Zilch, K., *The Effects of the Modified Composition of SCC on Shear and bond Behavior*. Ozawa, K. and Ouchi M. Editors, Proceedings of the second RILEM international symposium on self-compacting concrete Kochi University of Technology, Japan: COMS Engineering Corporation; 2001: pp. 501–506.
[15] Boel, V.; Helincks, P.; Desnerck, P. and Schutter, G., *Bond Behavior and Shear Capacity of Self-compacting Concrete*. Design, Production and Placement of self-consolidating concrete, RILEM Book Series 1, Khayat, K. H. and Feys, D. Editors, 2010: pp. 343-353.
[16] Teychenné, D. C.; Franklin, R. E. and Erntroy, H. C., *BRE Design of Normal Concrete Mixes*. 2nd Edition, Building Research Establishment, Watford, UK, 1997: 40 pp.
[17] Lachemi, M.; Hossain, K. M. A. and lambros, V., *Shear Resistance of Self-consolidating Concrete Beams – Experimental Investigations*. Canadian Journal of Civil Engineering, **32**, 2005: pp. 1103-1113.
[18] Hassan, A. A. A.; Hossain, K. M. A and Lachemi, M., *Behavior of Full-scale Self-consolidating Concrete Beams in Shear*. Cement and Concrete Composites, **30**, 2008: pp. 588-596.
[19] Hassan, A. A. A.; Hossain, K. M. A and Lachemi, M., *Strength, Cracking and Deflection Performance of Large Scale Self-consolidating Concrete Beams Subjected to Shear Failure*. Engineering structures, **32**, 2010: pp. 1262-1271.
[20] Japanese Society of Civil Engineering,*Specification for Design and Construction of Concrete Structures*. JSCE Standards, Part 1.
[21] Xue, X. and Seki, H., *Influence of Longitudinal Bar Corrosion on Shear Behavior of RC Beams*. Journal of Advanced Concrete Technology, **8**(2), 2010: pp. 145-156.
[22] Niwa, J., *Shear Equation of Deep Beams Based on Analysis*. Proceedings of JCI 2nd colloquium on shear analysis of RC structures, 1983: pp. 119-128.
[23] BS - EN 197-1, *Cement: Composition, Specifications, and Conformity Criteria for Common Cements*. 2000: 52 p.
[24] ASTM C618., *Specification for Fly Ash and Raw Calcined Natural Pozzolan for Use as a Mineral Admixture in Portland Cement Concrete*. Annual Book for ASTM Stand, **4**, 2000: 4p.
[25] ASTM C494., *Standard Specification of Chemical Admixtures for Concrete*. 1999: p. 9.
[26] Mphonde, A. G. and Frantz, G. C., *Shear Tests of High and Low Strength Concrete Beams Without Stirrups*. ACI Journal, Proceedings 81(4), 11984: pp. 350-356.